Mechanical analyses of a silicon micro propulsion system

Allegri G., Corradi S., Marchetti M., Tromboni P.D.

Aerospace and Astronautical Engineering Department, University of Rome "La Sapienza"
Via Eudossiana, 16 - 00184 Rome - Italy

ABSTRACT

This paper reviews the static analyses of a icromachined silicon structure, constituted of components realised by MEMS technology on silicon wafers. These structures have been studied using a FEM method and the results have been verified with a mesh-less method, which was implementd by a MATLAB code. The simulation results have demonstrated the limits of the analysed silicon structure and made possible the evaluation of the best bonding technologies in the specific application analyzed.

Keywords: MEMS, silicon-micromachined structures, bonding, FEM analysis, mesh-less method

NOMENCLATURE

MLS Moving Leas-Squares
u approximation function
p complete basis function
p vector of complete basis functions
a vector of unknown parameters
J weighted discerete norm
w weight function
W diagonal vector of weight functions
Φ shape function
Ω domain of neighborhood of a point
d nodal parameter
d nodal parameters vector
I node identifier
z_I distance from a simple point
z_{mI} domain of influence of node I
z_{cI} characteristic nodal spacing distance
z_{max} scaling parameter

I. INTRODUCTION

The new microsystem concepts are moving towards a decreasing of mass and dimension as evidenced by the aeorospace research activities under progress.

Generally the miniaturization of the structures makes the difference as well as the optimization of the materials and of the utilised technology. The challenge is to design products which are at the same time easy to develop and at elevated technical standards. The simulation is the first step of the design, but experimentation is the best method to test the systems reliability. Furthermore, MEMS technologies provide low costs in comparison with the technologies normally used for the realization of micromachined silicon stucture systems.

The silicon technology is actually used in aerospace, especially in propulsions, structures, and avionic field. Arrays of one-shot microthrusters in a three-layer sandwich configuration, electrically ignited, have been fabricated by Aerospace, TRW Inc., and the Californian Institute of Technology, in Pasadena [1]. Micrometrical scale pyrotechnic actuators for aerospace and medical application have been developed by DARPA [2]. A microthrusters array for small stationkeeping satellites has been developed by Aerospace and Astronautical Engineering Department and Electronics Department of “La Sapienza” University and G&A Engineering [3], [4].

II. CONFIGURATION

The silicon micromachined system fundamental concept consists of obtaining microstructures starting from silicon wafers {100} utilizing its surface, instead of its thickness. The test structure (like a thruster combustion chamber) is realised by etching a masked silicon wafer with KOH or TMAH [5].

This process allows to obtain different shapes both for vertical and horizontal walls, whose shape and dimensions can be varied in function of the operating conditions to which the system is dedicated for. The wall-shape depends on the choice of the crystallographic orientation of the wafer. Sample for testing can be seen in Figure 1, which shows the bonding surface.

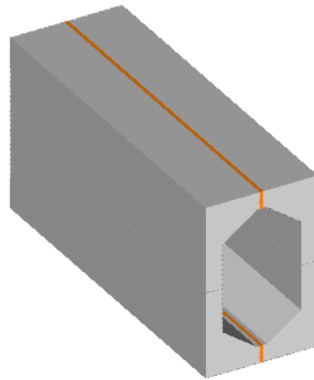

Fig. 1: *structure V-crack shaped used in the FEM simulation.*

In order to obtain a structure with a bonded surface and a discontinuous profile, simulating a crack geometry, two wafers processed in the same way are bonded together by the Silicon Direct Bonding process (SDB), which allows to form covalent bounds thanks to the contemporaneous use of pressure (atmospheric pressure or vacuum) and high temperature (1000 °C) or others techniques. Using 4 inches wafers and fixing the height of the structure equal to 1 cm, it is possible to obtain V-shaped cells 2 mm height and 4.74 mm wide, as shown in Fig. 2. This shape is due to the etching angle, technologically imposed as 54.74° for silicon wafer {100} [6]. The final structure, shown in Fig. 1, is obtained by cutting the wafer along its length, corresponding V-crack base.

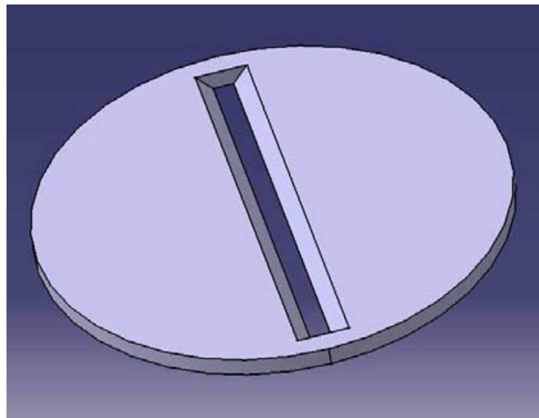

Fig. 2: *shape due to the eatching process in a masked wafer* **.**

III. THE SILICON AS STRUCTURAL MATERIAL

The crystalline silicon has a cubic atomic disposition with centered faces. This structure has crystalline plains with different characteristics, for this motive the silicon responds in different way to the mechanical loads or chemical eatching according to the wafer direction.

The deformation is not uniform in all directions because of the material anysotropy. This anysotropy is due to different crystallographic orientation.

Energetically, in an anysotropic material the energy accumulated by the material is redistributed not uniformly along the (1 0 0), (1 1 0) and (1 1 1) crystalline plains.

For a crystalline material with anysotropic mechanical properties, the Young modulus and the Poisson's coefficient are not enough to describe the elastic behavior of the material. The decreasing of the symmetrical material plains, the necessary parameters to describe the elastic behavior increase.

The characterization of crystalline silicon with a cubic centered faces structure needs three elastic constants and the constitutive relationships are represented by the following matricial expression:

$$\begin{Bmatrix} \sigma_x \\ \sigma_y \\ \sigma_z \\ \tau_{xy} \\ \tau_{xz} \\ \tau_{yz} \end{Bmatrix} = \begin{bmatrix} E_{11} & E_{12} & E_{12} & 0 & 0 & 0 \\ E_{12} & E_{11} & E_{12} & 0 & 0 & 0 \\ E_{12} & E_{12} & E_{11} & 0 & 0 & 0 \\ 0 & 0 & 0 & E_{44} & 0 & 0 \\ 0 & 0 & 0 & 0 & E_{44} & 0 \\ 0 & 0 & 0 & 0 & 0 & E_{44} \end{bmatrix} \cdot \begin{Bmatrix} \varepsilon_x \\ \varepsilon_y \\ \varepsilon_z \\ \gamma_{xy} \\ \gamma_{xz} \\ \gamma_{yz} \end{Bmatrix}$$

The parameters have the following values for a silicon wafer (1 0 0) oriented:

1. E_{11}=166 Gpa;
2. E_{12}= 64 Gpa;
3. E_{44}= 80 Gpa.

These values are very differents and the variation depend on many aspects, such as crystallographic orientation and temperature. The table 1 shows the different values of the principal mechanical properties of the silicon materials.

Crystal orientation	Young's modulus E [Gpa]	Shear modulus G [Gpa]	Temperature coefficient [10^{-6} K^{-1}]
[100]	166.0	79.0	-63
[110]	168.0	61.7	-80
[111]	186.5	57.5	-46

Table 1: *change in the silicon mechanical properties varying crystalloraphic orientation.*

VI. BONDING AND EATCHING

The bonding

The wafer bonding needs high quality in terms of planarity of the silicon wafer surface, because of that the cleaniless of the wafer is very important. The wafer surface must be clean removing:

1. particles like dust, hair, fibers;
2. organic contaminating like hydrocarbons coming from the air and from the wafers containers;
3. ionic contaminating like metallic ions coming from the containers in glass.

The remaining particles act as a spacer and inhibit the interactions between wafers bonded surfaces causing an incorrect adhesion. The organic contamination weakens the strength of the adhesion and they cause the formation of inclusion during the thermal treatment.
The metallic contaminants don't have effects on the strength of adhesion but they can influence the electric properties of the materials. As soon as the contaminants are removed, it needs to bond immediately, to minimize the wafer surface contamination. The bonding can be conducted by both manually and using commercial bonder. Different types of bonding techniques exist and have been examined:

Anodic Bonding. This process is used to bond a silicon wafer to a pirex wafer. Using temperatures up to 550 °Cs and by applying tensions up to 2000 Vs is obtained a chemical process that brings two materials in a permanent union.

Pressure Bonding. The mechanical pressure up to 400 kN and temperatures lower than 500°C are useful used to bond materials substrata using intermediary layers. Material like gold and glass are often used to encapsulate or to seal sensory in hollow.

Silicon Direct Bonding. The improvement of cleanig techniques and surface treatment permit the frequently use Silicon Direct Bonding. It essentially consists of two steps, the first, in which clean wafer is lined up and "pre-united", on temperature environemnt and both on void or atmospheric pressure conditions. The flollowing step consists of a high temperatures treatment to increase the adhesion energy. Conforming to the used bonding process and wafers surfaces aspect, the bond between the jointed surfaces can be two types. In the case of the ossidate wafers surface, the bond among two oxid layers ($SiO2$) is a Van der Waals bond, inter-molecular weak. In the case of the pure silicon wafers surfaces, the bond will be established among the same atoms of silicon, it will be strong covalent type. The bonding covalent type is generally obtained to elevated temperature, equal or upper than 1100°C: intermediary products can be produced at this high temperature and the quality of the bonding will decrease. An alternative way to obtain covalent bond is the combined use of ambient temperature and high vacuum.

The etching

The etching process is, generally used in electronic applications. It is possible with this process to remove some material from wide zones of a structure. The etching processes are grouped as follows into two classes: weat etching and dry etching.

*Wet etching***:** it is realized by dipping the wafers in a solution for the chemical attack maintained to assigned temperature. The characteristics of the solution determine the etching

time. Immediately after the extraction of the wafer from the solution, the wafer needs to be dipped into deionizated water to stop the removal process.

Dry etching: it is generally used for anysotropic materials. There are three known techniques of dry etching:

> *Plasma Etching*: the wafer surfaces, masking by photoresist, are struck by a gas, generally FREON, in a vacuum chamber. An electromagnetic field causes the ions bombardment responsible of the ablation of the silicon superficial layers.
>
> *Reactive etching:* is the combination of physical and chemical etching. This combines the energetic control of the ionic bombardment with the interaction of a chemical reaction.
>
> *Physical etching:* it is the use of particles to remove the material physically. A charged particles flow is directed toward the surface on which it intends to remove the material. This method is very close to the reacting etching, except for the use of the only energy for the motion of the ions toward the material to be removed.

The anisotropy of monocrystalline silicon influences the etching properties. A lot of the eatching products dissolve more quickly a crystalline plain than other. In the diamond silicon structure the{111} plain is more compact than {100} plain; therefore in the {100} plain the etching rate is lower than in the {111} plain. It is generally used the hydroxide of potassium in isopropanol (KOH-IPA) and the TMAH to etch silicon wafers. Unfrequently the hydroxide of sodium in isopropanol (NaOH-IPA) is used. In a silicon wafer {100} oriented and 4-6 Ohm resistivity, covered by a silicon oxide layer 1 μm thick, the concentrations that maximize the etching rate is 25% in weight of KOH and of 20% in weight of TMAH [7], [8].
The relation between the etching rates of the plans {100}and {111} is 100:1. The crystallographic orientation plains limits the obtainable angles by means the etching process. This angle varies from 0° to 90° respect to the crystal of silicon, but they reduce it, in the silicon wafers {100}, from 54.74° to 45.27°, respectively for the presence of the plains {111} and {110}.
The figure 3 shows the etching angle in a silicon wafer.

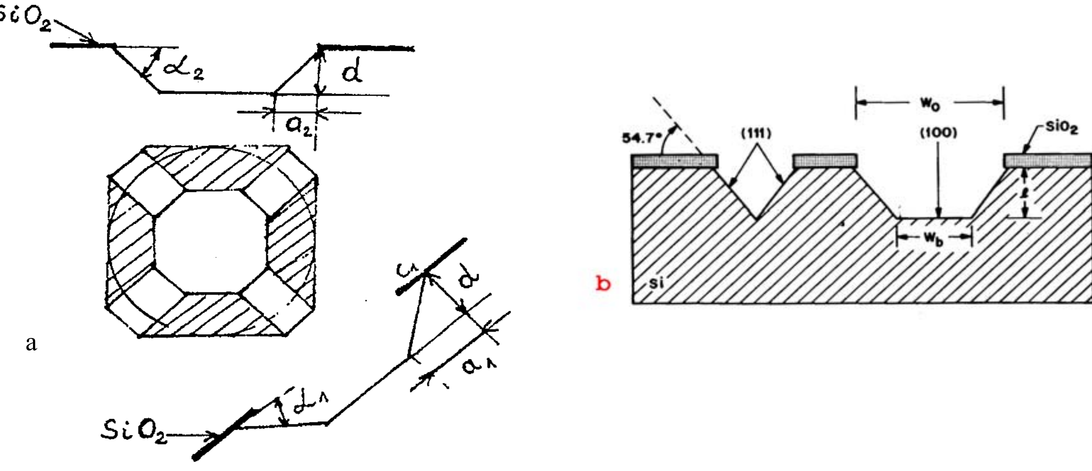

***Figura 3: a:** etching angle in a silicon crystal (α1: 45.27° ; α2: 54.74°) **b:** frontal view in a silicon wafer {100} after an etching process.*

V. STATIC ANALYSIS

A static analysis has been performed to verify that the pressure loads, considered acting to the internal wall of the structure, do not shatter the chamber walls. In fact, the silicon is not a typical structural material as shown in the precedent paragraph and it has a fragile behavior. The Young modulus of the silicon has been evaluated considering the orthotropic property of the silicon wafer used. In this analysis the influence has not been considered of the temperature on the mechanical prorperties of the silicon, also if this aspect can be very critical for space application.

Two FEM models have been realized using a FEMAP preprocessor. The first model, shown in figure 4, has been realized using plain strain elements, in order to predict the stress distribution in a middle transversal section and to permit the realization of a more accurate model. In this model the bonding has not been considered and the wafers surfaces have been considered perfectly adherent and continuous.
The second model, shown in figure 5, has been realized using 3D elements (8 nodes brick elments) in order to analyze also the shear stress along the depth of the structure, especially on the V-zone of the crack. The mesh has been increased in this zone, to verify the stress responsible to the crack opening.
Only half of the chamber has been considered due to the axial symmetry of the structure.

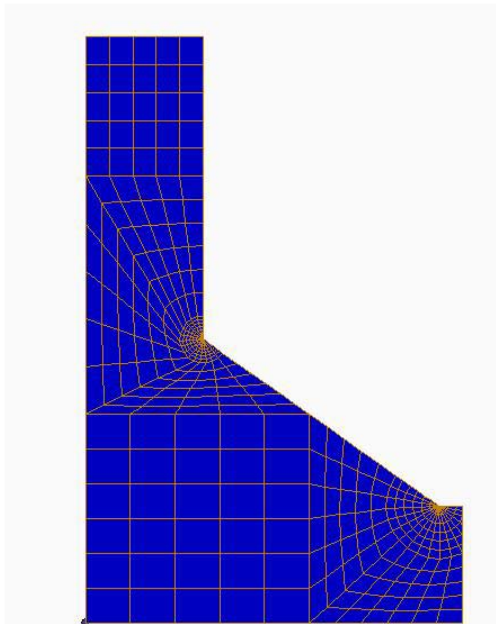

Fig. 4: *mesh plain strain for the 2D model*

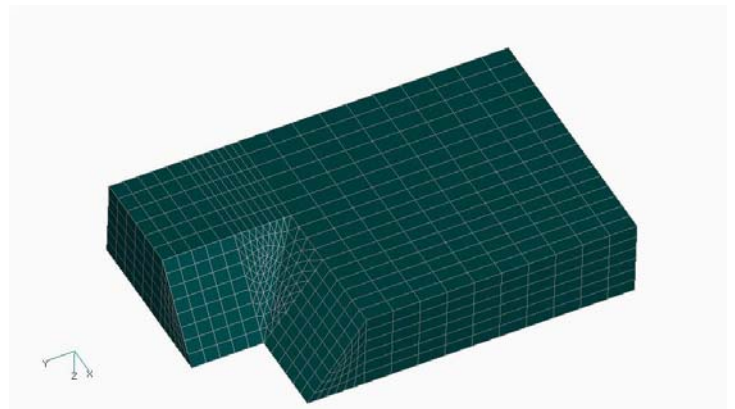

Fig. 5:*mesh brick for the 3D model*

The following constraint conditions have been imposed on the studied configuration:

- free at the far ends of the structure;
- the symmetric constraint along the lateral crack walls in order to simulate the presence of adjacent material;
- the z direction translation fixed in the middle transversal section.

According to this configuration, a 10 MPa pressure statically created on the inner wall of the both plain-strain and solid NASTRAN model. The figure 7 shows the constrain and load sets appplied to the 2D model. The chamber geometry predicts that the region most stressed is the wafer bounding surface, by the crack V-shaped tip. As aspected, figures 8 and 9 confirm that the bonding surface is the more stressed region. The stress values are in N/mm^2, with negative values depicting compressive stress and positive values depicting tensile stress. It can be seen that the maximum y normal stress value is close to 285.2 MPa and the total translation is equal to 5.05 µm, values very close to the debonding limit of the silicon wafers.
The reliability of results was very low, because of the limits of the used model, but the stress distribution has represented a good first step on which to build the second model.

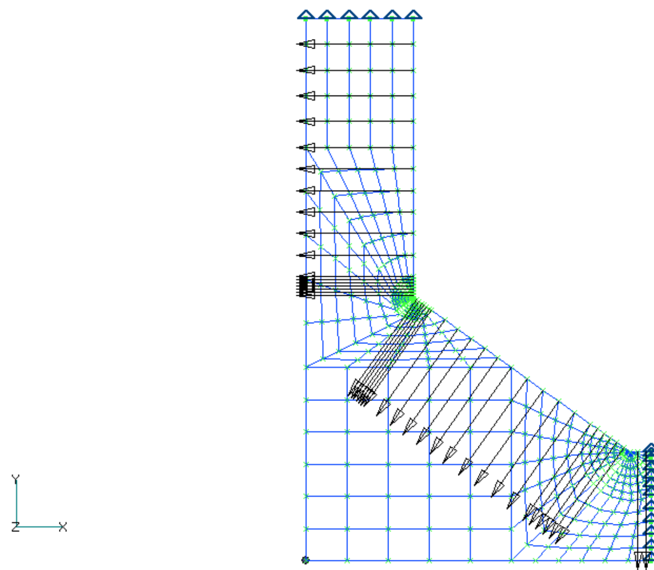

Fig. 7: *loads and constrains applied on the 2D FEM model*

The same pressure loads has been applied on the brick wall of the second model; the same boundary conditions used in the 2D model have been imposed. The figure 9 shows the obtained results on the brick model. It can be seen that the Von Mises Stress value in the middle section is close to 290 MPa and the total translation is equal to 5.89µm. These values are very similar to that obtained by the plain strain model. The brick model permits also to consider the boundary effect close to the far ends of the structure. At the boundary tips the stress are increased due to the boundary effects, as shown in the figure 9. The stress profile in the longitudinal elements (z direction) close to more stressed crack V-shape zone shows the stress values higher that in the structures middle sections.

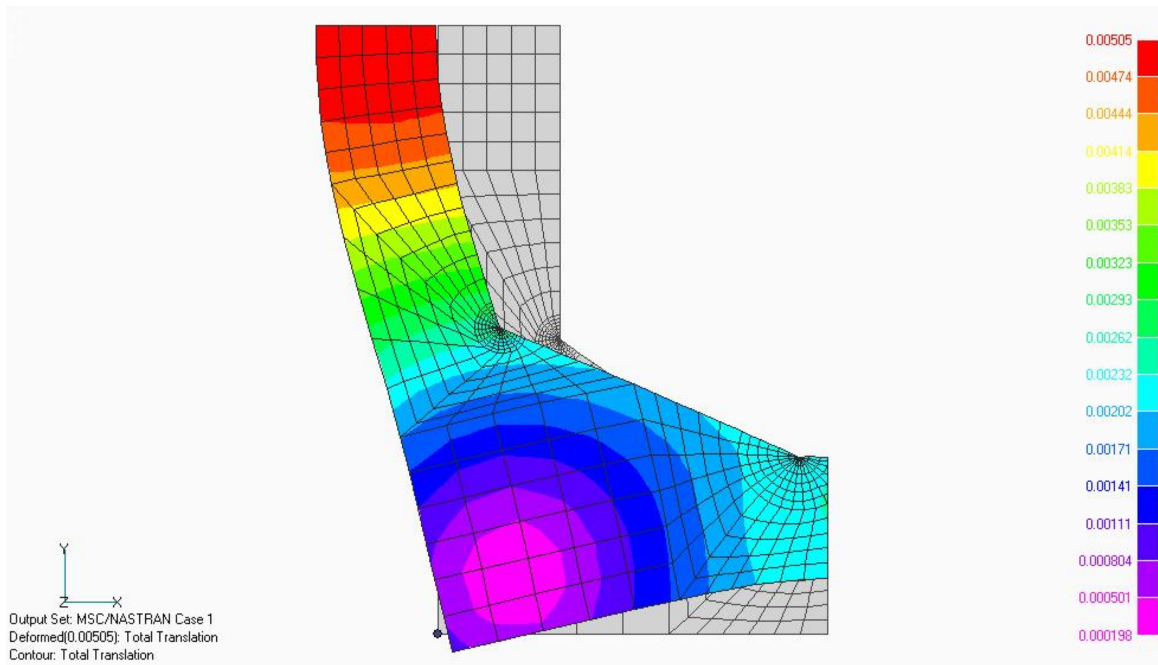

***Fig. 7:** total translation distribution in the plain strain model.*

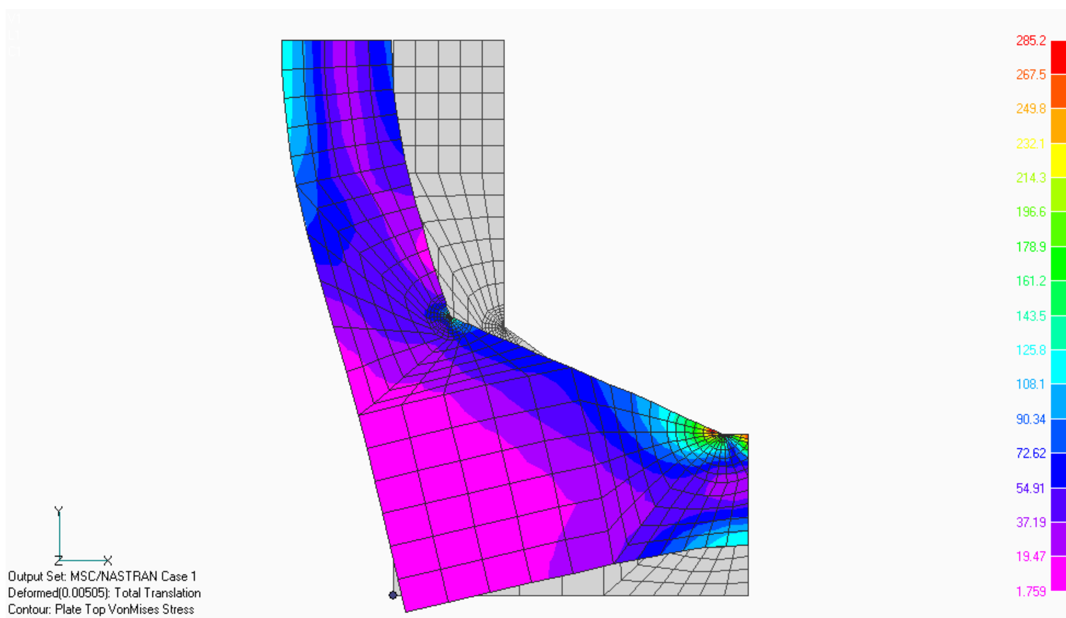

***Fig.8:** Von Mises stress distribution in the plain strain model. The undeformed configuration is visible.*

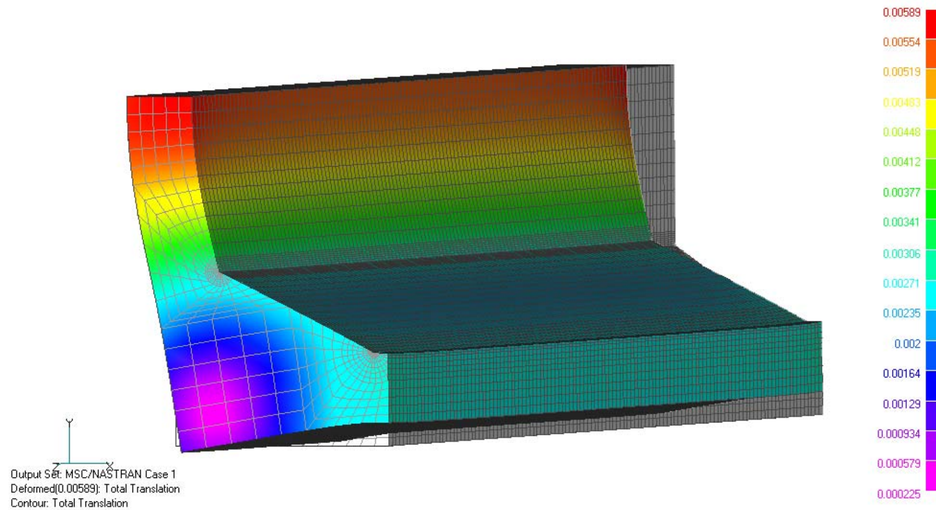

Fig. 9: *Total translation distribution in the brick model. The deformed configuration can be seen.*

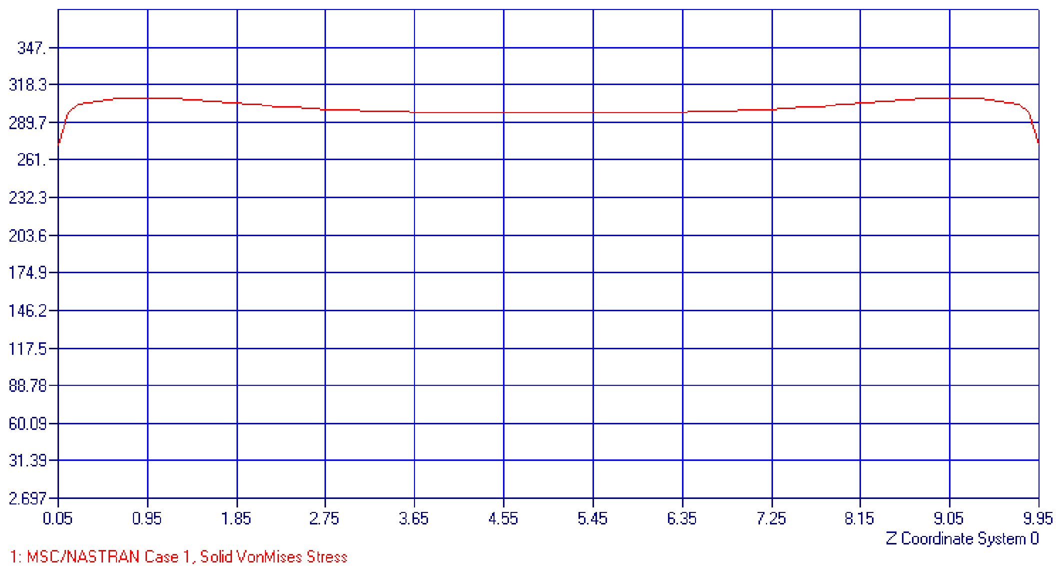

Fig. 10: *The Von Mises stress profile in the longitudinal elements (z direction) close to more stressed crack V-shape.*

VI. MESHLESS METHOD

In order to verify the NASTRAN analysis results a second code has been used. This code, developed by using a free-mesh concept, is particularly appropriate to the studied aplication, because is founded to a meshless method for analizing linear-elastic cracked structures subject to sinlge or mixed-mode loading conditions [9]. The method involves an element –free Galerkin formulation in conjuction with an exact implementation of essential boundary conditions. This method seems to solve the convenctional FEM limitations in solving solid mechanics problems characterized by a continous change in geometry of the domain under analysis. In fact, the FEM simulation of opening crack usually requires a large number of

remeshing to represent arbitrary and complex paths. Contrarily, the meshfree or meshless methods garanties significant potential for the moving boundary problem typified by growing cracks. This is made possible by the use of scattered set of nodal points in the domain of interest, witouht the necessity to employ structured mesh. A growing crack can be modeled by simply extending the free surfaces, which corresponds to the crack.
In the original EFGM meshless method [10], the meshless shape functions do not represent interpolation functions. Hence, the essential boundary conditions cannot be imposed exactly due to loss of Kronekcker-delta properties, so the general Lagrange multipliers approach needs to be employed to impose the boundary conditions. This requires solution of the Lagrange multipliers in addition to the discrete field varaibles. A modified method, based on a variational method in wich Lagrange multipliers are replaced by their physical meaning, has been introduced by Lu et al. [11]. An efficient formulation of the EFGM for fracture analysis of crack in homogeneous, isotropic, linear-elastic two-dimensional solids has been introduced [12] to involve enforcement of essential bundary conditions by a transformatoin method and a new weight function. If consider the function u(**x**) over a domain $\Omega \in R^k$, where k=1,2,3. Let $\Omega_x \subseteq \Omega$ denote a sub-domain describing the neighborhood of a point, $\mathbf{x} \in R^k$ located in Ω. The approximation, $u^h(\mathbf{x})$ of u(**x**) is:

$$u^k(x) = \sum_{i=1}^{m} p_i(x) a_i(x) = p^T(x) a(x)$$

where $\mathbf{p}^T(\mathbf{x})=\{\mathbf{p_1(x)}, \mathbf{p_2(x)},\ldots,\mathbf{p_m(x)}\}$ is a vector of complete basis functions of order *m* and $\mathbf{a(x)}= \{\mathbf{a_1(x)}, \mathbf{a_2(x)},\ldots,\mathbf{a_m(x)}\}$ is a vector of unknown parameters that depend on **x**. The basics functions should satisfy the following properties: $p_1(x)=1$, $p_i(x) \in C^s(\Omega)$, I=1,2,…,*m* where $C^s(\Omega)$ is a set of functions that have continuous derivatives up to order *s* on Ω, and $\mathbf{p}_i(\mathbf{x})$, i=1,2,…*m* constitute a lineraly independent set.
The basic function used is the following:

$$p^T(x) = \left\{1, x_1, x_2, x_1^2, x_1 x_1, x_2^2, \sqrt{2}\cos\frac{\vartheta}{2}, \sqrt{2}\sin\frac{\vartheta}{2}, \sqrt{2}\sin\vartheta\cos\frac{\vartheta}{2}, \sqrt{2}\cos\vartheta\sin\frac{\vartheta}{2}\right\} \quad (1$$

where *r* and θ are polar coordinates with the crack tip as the origin.
This expression has been used to capture the stress-singularity in linear-elastic fracture mechanism.

In equation 1) the coefficient vector, **a(x)** is determinated by minimizing a weighted discrete J norme defined as:

$$J(x) = \sum_{i=1}^{n} w_1(x)\left[p^T(x_1)a(x) - d_I\right]^2 = \left[Pa(x) - d\right]^T W\left[Pa(x)\right] - d \quad (2$$

where x_1 denotes the coordinates of node I, with $d_I=\{d_1, d_2, \ldots d_n\}$ with d_I representing the nodal parameter for node I, $W=\mathrm{diag}[w_1(x), w_2(x), \ldots w_N(x)]$, with $w_I(x)$ denoting the weight function associated with node I such that $w_I(x) \geq 0$ for all **x** in the suport Ω_x for wich $w_1(x)$ and zero otherwise, *n* is the number of nodes in Ω_x for wich $w_I(x)>0$, and:

$$P = \begin{bmatrix} p^T(x_1) \\ p^T(x_2) \\ \\ p^T(x_n) \end{bmatrix}$$

Using these equations we can obtain:

$$u^h(x) = \sum_{I=1}^{n} \Phi_I(x) d_I = \Phi^T(x) d \qquad (3$$

where

$$\Phi^T(x) = \{\Phi_1(x), \Phi_2(x), ..., \Phi_n(x)\} \qquad (4$$

is a vector with its Ith component:

$$\Phi_I(x) = \sum_{j=1}^{m} p_j(x) \left[A^{-1}(x) C(x)\right]_{jI} \qquad (5$$

representing the shape function of the MLS approximation corresponding to node I.
The most important choice in the less-mesh method is to identify the weight function, w(x), because it value can affect the MLS approximation of $u^h(x)$.
The following weight function has been used :

$$w_I(x) = \begin{cases} \dfrac{\left(1 + \beta^2 (\frac{z_1^2}{z_{mI}^2})\right)^{((1+\beta)/2)} - \left(1+\beta^2\right)^{-((1+\beta)/2)}}{1 - (1+\beta^2)^{-(1+\beta)/2}} & z_I \le z_{mI} \\ 0 & z_I > z_{mI} \end{cases} \qquad (6$$

where β is the parameter controlling the shape of the weight function, $z_I = ||x - x_I||$ is the distance from a sampling point, x to a node x_I, z_{mI} is the domain of influence of node I such that

$$z_{mI} = z_{\max} z_{cI} \qquad (7$$

in wich z_{cI} is a characteristic nodal spacing distance and z_{max} is a scaling parameters.

The geometry described in the abouve aragraphe has been analised also using the mesh-less method. The figure 11 shown the undeformed and the deformed configuration.

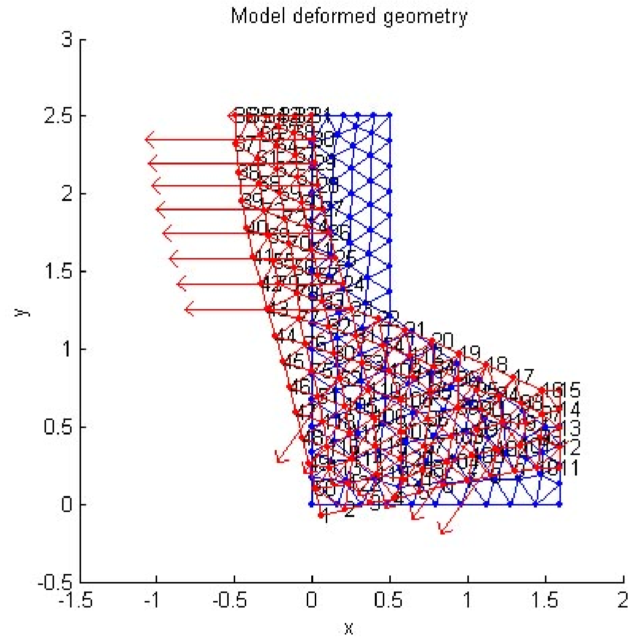

Fig. 11*: meshless deformed picture of the deformed plain stress model in the mesh-less method.*

The static analysis has been performed and the results have according to FEM results. The figure 12 shows the obtained total translation distribution. It was very close to the total translation distribution obtained with FEM models. It can be see that the maximum total translation value is equal to 5.4 µm. the Von Mises stress value is close to 277 Mpa.

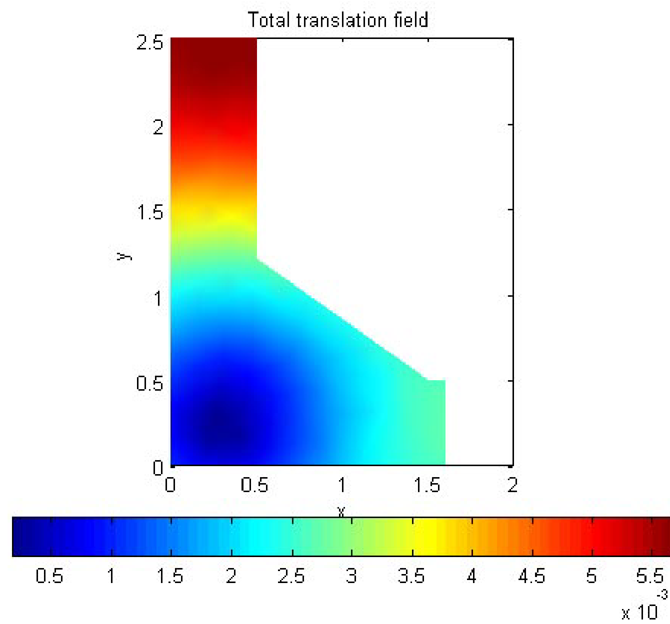

Fig. 12*: total translation distribution on the deformed plain stress model unsing the mesh-less method.*

VII. CONCLUSION

In this paper a cracked structure has been simulated by FEM and meshless method. A static analysis has been performed to verify the performances of the system in operating conditions and to compare the results obtained by the different used methods. Also the properties silicon wafer and the eatching and bonding processes have been considered to performe the static analysis The results obtained by FEM and meshless method are in agreement between them, demonstrating the consistency of the used models.
These data can be verify through the experimental set-up.

ACKNOWLEDGMENT

The authors wish to thank the full professor A. Ferrari and prof. M. Balucani (Electronics Engineering Department – DIE- of "la Sapienza" University) for many useful discussion concerning this research, as well as the study of the structure V-shape using etching silicon techology. This work has been realised in the frame of the SMART (Small Motor AeRospace Technology) contract, founded by ASI and developed in collaboration with G&A Engeneering.

REFERNCES

[1] D. Lewis, S. Janson, R. Cohen and E. Antonsson, "Digital MicroPropulsion" Sensorsand Actuators A: Physical, 2000, 80(2) pages 143-154.

[2] Carole Rossi, Daniel Estève and Corinne Mingués, "Pyrotechnic actuator: A new generation of Si integrated actuator," European Materials Research Society (E-MRS) meeting, Strasbourg, France, 16-19 June 1998.

[3] Lamedica G., Balucani M., Tromboni P.D., Marchetti M., Ferrari A., "Microthrusters in Silicon for Aerospace Application", IEEE Aerospace and Electronic Systems, September 2002, ISSN 0885-8985, Vol.17, n°9.

[4]

[5] Engineered Materials Handbook, vol.4,1991 ASM Handbook Properties and Selection, Non ferrous Alloys and Special Pourpose Materials, 1990

[6] I. Barycka, I. Zubel, "Silicon anisotropic etching in alkaline solutions I, The geometric description of figures developed under etching Si(100) in various solutions. *Sensor and Actuators Ak, v.70, p.250-259,* 1998

[7] I. Baraycka, I. Zubel: Silicon anisotropic etching in KOH-isopropanol etchant; Sensors and Actuators A **48** (1995) 229

[8] N. Rao, S. Rahman, "An efficient meshless method for structure analysis of cracks, Computational Mechanics 26 (2000) 398-408

[9] Belytshko T, Lu YY, Gu L (1994) Element free Galerkin methods. Int. J. Numer. Meth. Engng 37:229-256.

[10] Lu YY, B elytshko T, Gu L (1994) A new implementation of the element free Galerkin method. Comp. Meth. Appl. Mech. Engng 113: 397-414

[11] Rao B.N., Rahman S., An efficient meshless method for fracture analysis of cracks, Computational Mechanics 26 (2000) 398-408

Figure captions

Fig. 1: *structure V-crack shaped used in the FEM simulation.*

Fig. 2: *shape due to the eatching process in a masked wafer .*

Fig. 3: a: *etching angle in a silicon crystal (α1: 45.27° ; α2: 54.74°)* ***b:*** *frontal view in a silicon wafer {100} after an etching process.*

Fig. 4: *mesh plain strain del modello 2D*

Fig. 5:*mesh brick del modello 3D*

Fig. 6: *loads and constrains applied on the 2D FEM model*

Fig. 7: *total translation distribution in the plain strain model.*

Fig. 8: *Von Mises stress distribution in the plain strain model. The undeformed configuration is visible.*

Fig. 9*: Total translation distribution in the brick model. The deformed configuration can be seen*

Fig. 10*: The Von Mises stress profile in the longitudinal elements (z direction) close to more stressed crack V-shape.*

Fig. 11*: meshless deformed picture of the deformed plain stress model in the mesh-less method.*

Fig. 12*: total translation distribution on the deformed plain stress model unsing the mesh-less method.*